Contents

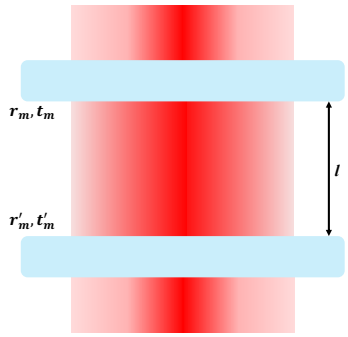

(a) Broadband cavity.

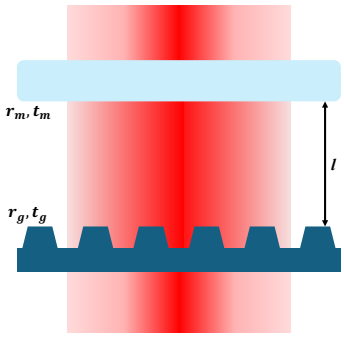

(b) Single Fano cavity.

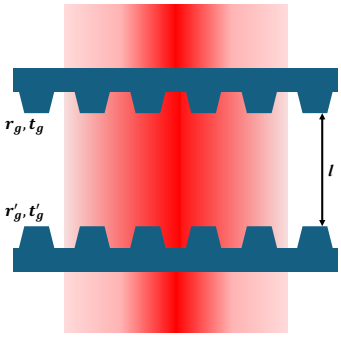

(c) Double Fano cavity.

1 Introduction

2 Theory

2.1 An Optical Cavity

An optical cavity is generally comprised of two highly reflective optical resonators. It is used for trapping any amount of light for an extended period of time, thus increasing the effective cross section of a given interaction between some object and the field inside the cavity.

Another attribute of the optical cavity is that it gives rise to so-called eigenstates related to the length of the cavity[1]. As the cavity does not expand infinitely, the allowed modes inside the cavity are limited to ones which fulfill the identity [2]

$$2d\cos\theta = m\lambda. \tag{1}$$

Here d is the length of the cavity, θ is the incidence angle of the light coupling into the cavity, λ is the wavelength of the light and $m = 1, 2, 3, ...$ is a positive integer describing the order of the mode. For the rest of this thesis it will be assumed that the laser couples into the cavity at normal incidence, meaning that $\theta = 0°$ and thus $\cos\theta = 1$.

2.1.1 The Fundamental Mode: A Gaussian Beam in the Large Waist Approximation

In order to describe the allowed modes within an optical cavity, it is first assumed that a single-mode field is linearly polarized. We then consider solutions to the wave equation

$$\nabla^2\vec{E} = \frac{1}{c^2}\frac{\partial^2\vec{E}}{\partial t^2}, \tag{2}$$

given as

$$\vec{E} = E_0(x, y, z)\vec{\epsilon}e^{ikz}. \tag{3}$$

Here $E_0(x, y, z)$ describes the electric field amplitude, $\vec{\epsilon}$ is denoted the polarization vector and $k = 2\pi/\lambda$ is the angular wave number of the field propagating along the z-axis. It is assumed that the electric field has a Gaussian transverse distribution[1].

[1]When this is the case, the laser is said to operate in the lowest possible mode denoted TEM_{00}. This implies the assumption of ideal lasing conditions.

This is almost the simplest description of the propagating field, however, as the spacial dependence of the field amplitude still might cause problems, we consider the range in which this can be neglected.

It can be shown from the derivation of the Gaussian distribution that the waist of the beam $w(z)$, which depends on the spacial coordinate in the direction of propagation, can be described as [1]

$$w(z) = w_0\sqrt{1 + \left(\frac{z}{z_R}\right)^2}, \tag{4}$$

where z is the distance from focus, w_0 is the beam waist at focus and z_R is the so-called *Rayleigh range*. The Rayleigh range describes the range in which the beam diverges slowly, whereas after this has been surpassed, the beam will begin to diverge more rapidly. By quick inspection of eq. (4) it is seen that

$$w(z) = \begin{cases} w_0, & \text{for } z = 0 \\ w_0\sqrt{2}, & \text{for } z = z_R, \end{cases} \tag{5}$$

which shows that the beam waist diverges no more than by a factor of $\sqrt{2}$ from the optimal case, for $0 \leq z \leq z_R$. Considering the case where $z \neq 0$ but however much smaller than the Rayleigh range z_R, we can further inspect eq. (4) and find that this leads to negligible changes in the waist of the beam. Specifically, it can fairly easily be seen that

$$\left(\frac{z}{z_R}\right)^2 \approx 0, \quad \text{for } z << z_R \tag{6}$$

which in turn leads to

$$w(z) \approx w_0. \tag{7}$$

The Rayleigh range can be written as [2]

$$z_R = \frac{\pi w_0^2}{\lambda}, \tag{8}$$

which, through the exponential dependence on w_0, shows that a large beam waist will result in a long Rayleigh range. As an example, consider

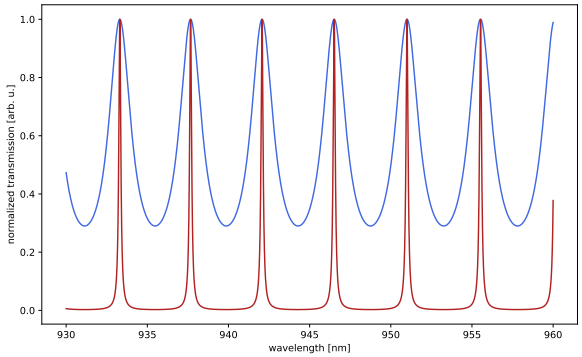

Figure 2: Comparison of an arbitrary Fabry-Perot cavity of high and low finesse, respectively. The high finesse cavity and a reflectivity of $|r|^2 = 0.90$, while for the low finesse cavity $|r|^2 = 0.30$.

a beam of waist $w_0 = 200\mu m$ and wavelength $\lambda = 950nm$. This would result in a Rayleigh range of $z_R = 13.23cm$.

Finally we can conclude, that any optical cavity, for which the total distance travelled inside the cavity[2], is significantly shorter than the Rayleigh range of the incident beam, the spacial dependence of the field amplitude inside the cavity is negligible, and the fundamental mode can be described simply by a linearly polarized plane wave

$$\vec{E} = E_0 \vec{\epsilon} e^{ikz}. \tag{9}$$

This is often referred to as the *large waist approximation* of a Gaussian beam, due to the dependence on w_0 of eq. (8).

2.1.2 The Fabry-Perot Interferometer

2.2 The Fano mirror: a sub wavelength grating

2.2.1 Geometric optical analysis

Considering an ideal grating with period d in the sub-wavelength regime, it can be shown that only a single mode of reflection/transmission is supported.

[2]For any optical cavity the incident light will travel a distance inside the cavity according to, not only the length of the cavity, but also the amount of round trips the light makes when confined inside the cavity.

Any grating, of arbitrary dimensions, must comply with the very general *grating equation*[2] given as

$$\sin\theta_m = m\frac{\lambda}{d}, \tag{10}$$

for the special case of a linearly polarized plane wave incident on a grating placed normal to the direction of propagation. Now, inserting the sub-wavelength condition $d \ll \lambda$, it is easily seen that the right side of the equation blows up for any order of reflection $|m| > 0$, effectively showing that this is the aforementioned single supported mode in this regime. Furthermore, it can be equally easily seen that the propagation direction of the 0'th order mode is the same as the incident beam, i.e. normal to the grating.

2.2.2 Reflection/transmission spectra and line shape analysis

2.2.3 Lossless grating

We wish to analytically describe the wavelength-dependent spectra for the transmission and reflectivity of an infinite sub-wavelength grating. By first considering the case where absorption and thermal coupling effects are neglected, i.e. a lossless grating, we can assume conservation of energy and thereby the relations

$$|r_g|^2 + |t_g|^2 = 1 \quad \text{and} \quad |r_d|^2 + |t_d|^2 = 1, \tag{11}$$

where the subscripts g and d indicate the *grating* and *direct* transmissions and reflectivities, respectively. It is implied that the direct coefficients are constants and describe the transmission and reflectivity when the incident wavelength is significantly detuned from any guided-mode resonance of the grating. Furthermore, it is also implied that the grating coefficients are functions of the incident wavelength.

We now assume a normal incident beam on the grating as a linearly polarized monochromatic plane wave, with a wavelength close to a guided-mode resonance of the grating. In order to describe the coefficients r_g and t_g we follow the formalism presented by Fan and Joannopoulos [3] and consider the likely paths of the incident light through the grating. It is

quite intuitive to consider the case where the light is simply transmitted, and this shall be our first case hereafter denoted the *direct pathway*. Another case one might consider is the one where the incident light excites the guided-mode resonance in the grating, thus causing interference. This case is denoted the *indirect pathway* and decays more slowly than it's direct counterpart.

The interference caused when the guided mode is excited is often referred to as *Fano resonances*, due to its physical similarities to the description of interference between a discrete autoionized state and a bound continuum state first reported by Fano [4]. The cross section of inelastic scattering, when measured as a function of energy, showed characteristic asymmetric peaks. These were described as the aforementioned interference pattern between *direct* (the discrete state) and *indirect* (the continuum state) pathways.

By generalizing the model of Fan and Joannopoulos [3] we describe the transmission and recletivity coefficent amplitudes as

$$r_g = r_d + \frac{a}{k - k_1 + i\gamma} \quad \text{and} \quad t_g = t_d + \frac{b}{k - k_1 + i\gamma}, \tag{12}$$

where $k = 2\pi/\lambda$ is the incident wave number, $k_1 = 2\pi/\lambda_1$ is the wave number according to the guided-mode resonance and γ is the HWHM (half width at half maximum) of the guided-mode resonance. Complex coefficients a and b describe the interference between the directly transmitted or reflected waves and the guided mode of the grating.

Note that in eq. (12) the right side of the expression for each coefficient corresponds to the continuum state i.e. the indirect pathway, while the direct transmission and reflection coefficients take the role of the autoionized discrete state, i.e. the direct pathway[3] [4]

As we are dealing with an ideal, lossless, grating, we assume coefficients a and b to be equal, meaning that we specifically assume vertical symmetry

[3]The general eigenvector of a state comprised of a super-position between a discrete state and a continuum, i.e. a state vector corresponding to a Fano resonance, is given as $\Psi_E = a\phi + \int dE' b_{E'} \psi_{E'}$, given in eq. (2) in ref. [4], where a and $b_{E'}$ describes the probability of either pathway.

throughout the grating. By considering eq. (11) this in turn leads to

$$a = b = -i\gamma(t_d + r_d), \tag{13}$$

which further yields an expression for the grating transmission amplitude coefficient on the form

$$t_g = t_d \frac{k - k_0}{k - k_1 + i\gamma}. \tag{14}$$

Here, the newly introduced $k_0 = 2\pi/\lambda_0$ is the zero-transmission/unity-reflectivity wave number.

To generalize eq. (14) to include non-unity reflectivity and non-zero transmission, we allow for $a \neq b$ meaning that the case of vertical asymmetry is included in the model. By assuming $r_d, t_d \in \mathbb{R}$, eq. (11) leads to the coupled differential equations

$$\begin{aligned} &t_d x_a + r_d x_b = 0, \quad \text{and} \\ &x_a^2 + y_a^2 + x_b^2 + y_b^2 + 2t_d\gamma y_a + 2r_d\gamma y_b = 0, \end{aligned} \tag{15}$$

where $\{x, y\}_{a,b}$ respectively denotes the real and imaginary parts of the coefficients a and b. Solving eqs. (15) leads to the correct complex reflectivity coefficients and the expression for the transmission coefficient amplitudes now reads

$$t_g = t_d \frac{k - k_0 + i\beta}{k - k_1 + i\gamma}, \tag{16}$$

where k_0 and β are defined from the expression for a found by solving eqs. (15), given as

$$a = t_d(k_1 - k_0 - i\gamma + i\beta). \tag{17}$$

Finally, this allows for non-zero transmission and non-unity reflectivity at wave number k_0.

2.2.4 Lossy grating

In order to modify the above model such that losses, e.g. due to absorption or thermal coupling effects, are accounted for, we add a resonant loss term to the energy conservation relation in eq. (11). For this we introduce

the resonant loss level L, which must be known in order to accurately calculate the complex reflectivity coefficients. The energy conservation relation is modified such that

$$|t_g|^2 + |r_g|^2 + \frac{c^2}{(k-k_1)^2+\gamma^2} = 1, \tag{18}$$

where the coefficient $c^2 = L((k-k_1)^2+\gamma^2)$ includes the resonant loss term L. A new set of coupled differential equations are found, using eq. (18), given as

$$\begin{aligned} &t_d x_a + r_d x_b = 0, \quad \text{and} \\ &x_a^2 + y_a^2 + x_b^2 + y_b^2 + c^2 + 2t_d\gamma y_a + 2r_d\gamma y_b = 0. \end{aligned} \tag{19}$$

It is easily identified that eq. (15) and eq. (19) differ only by the addition of coefficient c^2, and thereby the losses. Solving eq. (19) leads to the correct complex reflectivity coefficients, except that they now account for any losses associated with the grating.

In conclusion, the complete grating model consists of an expression for the transmission coefficients and a set of coupled differential equations for the reflection coefficients, shown in eq. (16) and eq. (19), respectively. The model on the form used for this project and subsequent thesis is derived in previous work by A. Darki et al. [5] and more recently T. Mitra et al. [6].

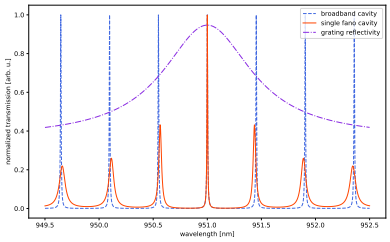

(a) 1000um fano and broadband cavities.

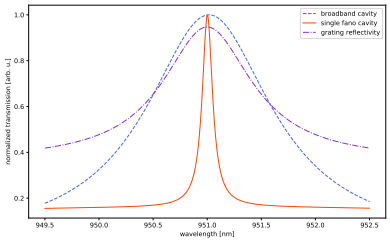

(b) 5um fano and broadband cavities.

2.3 The Fano cavity

2.3.1 The single Fano cavity: broadband mirror + fano mirror

Figures:

- Transmission of single fano and broadband cavities (long cavity - not in fano regime) (fig. 2a in 2018 paper)
- Transmission of single fano and broadband cavities (short cavity - in fano regime) (fig. 2b in 2018 paper)
- Analytical linewidth as a function of cavity length.

2.4 The double Fano cavity: two fano mirrors

2.4.1 The double fano transmission model

2.4.2 Comparison between the double fano, single fano and broadband cavities (lossless + symmetric)

Figures:

- resonance peaks of all three cavities (maybe intracavity for easier comparison).
- Off-resonance trans. of all three cavities (maybe only single and double)
- linewidth as a function of cavity length of all three.

2.4.3 Transmission as a function of losses (symmetric double fano cavity)

Figures:

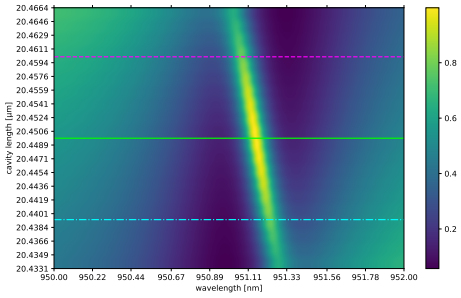

(a) cmap showing transmission as a function of wavelength for cavity lengths ranging $l_g \to l'_g$.

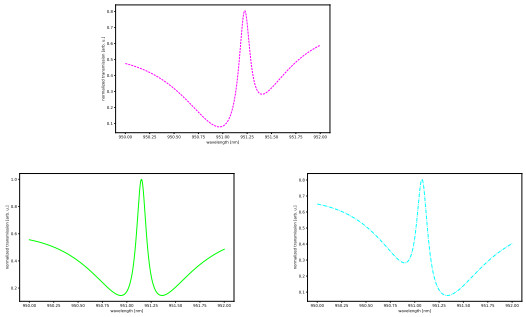

(b) Slices of the cmap showing the optimal length and wavelength of double fano cavity (lossless). Magenta = 71.3pm, cyan = 71.3pm and lime = 58.6pm.

- Trans. spectra for different values of L.
- linewidth as a function of L. (plot den analytiske linjebredde sammen med)

2.4.4 Spacial and spectral detuning - $l_g \geq l \geq l'_g$ & $\Delta \neq 0$ (lossless double fano cavity)

Figures (spectral detuning):

- Constructed grating trans. spectra (showing the result of varying only the spectral parameters of one grating, λ_0 and λ_1).
- Full range cavity transmission spectra of single + double fano cavities with grating transmission (note: resonance peak is between the trans. minima of the two gratings).
- Cavity trans. spectra for different values of Δ (constant cavity length).
- Linewidth as a function of spectral detuning Δ.

Figures (spacial detuning):

- Cavity trans. spectra for different lengths (small/large detuning comparison).
- Linewidth as a function of cavity length ($l_g \to l'_g$).

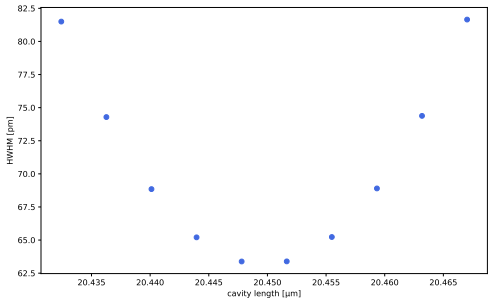

Figure 5: intracavity linewidth as a function of cavity length (same cavity as depicted in cmap above.)

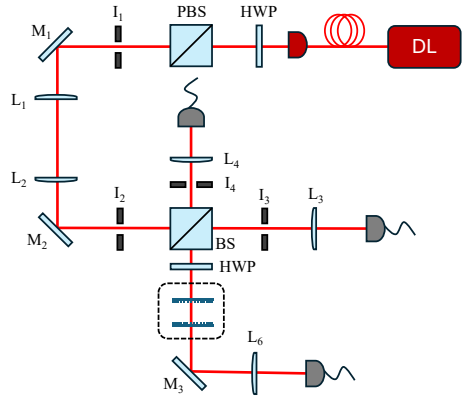

(a) Schematics of the experimental setup for measuringthe transmission through a double fano cavity. The cavity setup shown in (b) is located in position marked by the dotted line.

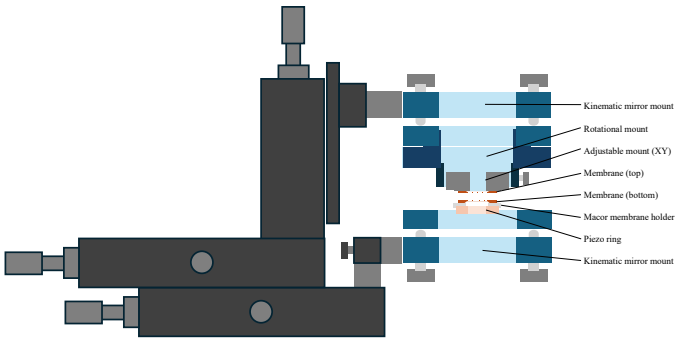

(b) Sketch of the part of the experimental setup containing the optical cavity.

Method

3 Method

3.1 The experimental setup

3.2 Characterization of sub-wavelength grating

Figures:

- Pictures of the membrane before patterning.
- AFM profile of the grating after patterning. (talk about profilometry and the physical parameters of the grating and their meaning for project).
- MAYBE: MIST simulation showing that the model accurately pre-

dicts the simulated spectra.

3.2.1 Obtaining normalized transmission/reflection spectra

3.2.2 Adjusting the beam waist - the optical telescope

3.2.3 The alignment procedure

3.2.4 Normalization

3.3 Cavity measurements

3.3.1 Determining the cavity length from the FSR

Figures:

- Linewidth as a function of "time" - to see the reduction of the linewidth as the piezo reaches an equilibrium where any time-dependent drift is reduced.

3.3.2 Normalization

3.3.3 Single fano cavity characterization

3.3.4 Aligning the cavity

Incluce:

- Scan for optimal cavity length
- Measure the spectral linewidth
-

3.3.5 Double fano cavity characterization

3.3.6 Off-resonance Fabry-Perot cavity (alignment technique)

3.3.7 Centering of the top grating (pinhole method)

3.4 Parallelism study (deviation from normal incident)

Results

4 Simulations

4.1 The single Fano cavity

4.2 The double Fano cavity

Figures:

- Simulated spectra of M3 and M5.
- Simulated length scans of M3 and M5.
- M3/M5 cavity trans. spectra (on resonance + full range)

  for lengths: $l_{M3} \rightarrow l_{M5}$

  for length: $l = 1/2 \cdot (l_{M3} + l_{M5})$
- Optimal result comparison with single fano/broadband cavities of similar losses.
- Optimal result comparison with the ideal case from prev. section.
- Simulated linewidth as a function of cavity length (include the same for broadband and single fano cavities).

5 Experimental results

5.1 The single Fano cavity

Figures:

- Single fano cavity transmission as a function of wavelength.
- Short scan of the single fano cavity tranmission, with found linewidth.
- Long scan Fabry-Perot fringes for determining FSR -> cavity length.
- linewidth as a function of cavity length (compare with broadban cavity).

5.2 The double Fano cavity

5.2.1 Realizing the double fano model

Figures:

- Fit of the double fano model (long + short cavity)

5.2.2 Double fano off-resonance Fabry-Perot cavity

Figures:

- Off-resonance double fano transmission as a function of wavelength (show that the off resonance transmission goes close to 100 percent for a well-aligned cavity).

5.2.3 The double fano linewidth

Figures:

- "Semi-short" scan data, fit to the double fano transmission model.
- Short scan data, fit to the Fano function (for measuring linewidth).
- Linewidth as a function of cavity length (compare double fano, single fano and broadband cavitites).

6 Discussion

6.1 Optimal configuration for double fano cavity - spacial limitation for the cavity length

6.2 Spacial drift of the piezo ring

6.3 Noise reduction - coupled/uncoupled mechanical/acoustic vibration (the plexi-glass box)

6.4 Broadening sources (especially for long cavities)

6.5 Improvements to the setup

7 References

[1] Marc Eichhorn. *Laser Physics - From Principles to Practical Work in the Lab*. Springer International Publishing Switzerland, 2014.

[2] Frank L. Pedrotti, Leno M. Pedrotti, and Leno S. Pedrotti. *Introduction to Optics, 3rd edition*. Cambridge University Press, 2018.

[3] Shanhui Fan and J. D. Joannopoulos. "Analysis of guided resonances in photonic crystal slabs". In: *Physical Review B* 65 (2002).

[4] U. Fano. "Effects of Configuration Interaction on Intensities and Phase Shifts*". In: *Physical Review* 124.6 (1961).

[5] Ali Akbar Darki. "Nanostructured tramplines for photonics and sensing". PhD thesis. Department of Physics and Astronomy - Aarhus University, 2022.

[6] T. Mitra et al. "Narrow-linewidth Fano microcavities with resonant subwavelength grating mirror". In: *Optics Express* 32.9 (2024).